Trends of daily peak wind gusts in Spain and Portugal, 1961–2014

Cesar Azorin-Molina[1], Jose-A. Guijarro[2], Tim R. McVicar[3,4], Sergio M. Vicente-Serrano[1], Deliang Chen[5], Sonia Jerez[6], and Fátima Espírito-Santo[7]

[1]Departamento de Procesos Geoambientales y Cambio Global, Instituto Pirenaico de Ecología, Consejo Superior de Investigaciones Científicas (IPE-CSIC), Zaragoza, Spain, [2]State Meteorological Agency (AEMET), Delegation of the Balearic Islands, Palma de Mallorca, Spain, [3]CSIRO Land and Water, Canberra, ACT, Australia, [4]Australian Research Council Centre of Excellence for Climate System Science, Sydney, New South Wales, Australia, [5]Department of Earth Sciences, University of Gothenburg, Gothenburg, Sweden, [6]Department of Physics, University of Murcia, Murcia, Spain, [7]Instituto Português do Mar e da Atmosfera, Lisboa, Portugal

Abstract Given the inconsistencies of wind gust trends under the widespread decline in near-surface wind speed (stilling), our study aimed to assess trends of observed daily peak wind gusts (DPWG) across Spain and Portugal for 1961–2014 by analyzing trends of (i) the frequency (90th percentile) and (ii) the magnitude (wind speed maxima) of DPWG. Wind gust series were homogenized on a daily basis, using MM5-simulated series as reference, resulting in 80 suitable station-based data sets. The average DPWG 90th percentile frequency declined by -1.49 d decade^{-1} ($p < 0.05$) annually. This showed marked seasonal differences: decreasing in winter (-0.75 d decade^{-1}; $p < 0.05$) and increasing in summer ($+0.18$ d decade^{-1}; $p > 0.10$). A negligible trend was calculated for the annual magnitude of DPWG (-0.005 m s^{-1} decade^{-1}; $p > 0.10$), with distinct seasonality: declining in winter (-0.168 m s^{-1} decade^{-1}; $p < 0.10$) and increasing in summer ($+0.130$ m s^{-1} decade^{-1}; $p < 0.05$). Combined, these results reveal less frequent and declining DPWG during the cold semester (November–April) and more frequent and increasing DPWG during the warm semester (May–October). Large-scale atmospheric changes such as the North Atlantic Oscillation Index (negative correlations ~ -0.4–-0.6; $p < 0.05$) and the Jenkinson and Collison scheme (positive correlations mainly with Westerly regime: $\sim +0.5$–0.6; $p < 0.05$) partly account for the decadal fluctuations of both frequency and magnitude of DPWG, particularly in winter. However, the North Atlantic Oscillation index-DPWG relationships are smaller in spring, summer, and autumn (~ -0.1–-0.2; $p > 0.10$), especially for the frequency, suggesting the role of local-to-mesoscale drivers.

1. Introduction

Most studies dealing with climate variability of near-surface wind speed analyzed long-term trends from daily mean wind speed [*McVicar et al.*, 2012]. Overall, these investigations have reported a widespread decline in measured near-surface wind speed (termed "global stilling") [*Roderick et al.*, 2007] in many locations (especially midlatitudes regions) such the United States [*Pryor et al.*, 2009], China [*Guo et al.*, 2011], Australia [*McVicar et al.*, 2008], Czech Republic [*Brázdil et al.*, 2009], and Iberian Peninsula [*Azorin-Molina et al.*, 2014] (see *McVicar et al.* [2012] for a comprehensive review). Under this terrestrial stilling the study of daily peak wind gust (hereafter DPWG) speed has only received minimal attention during the last two decades. The state of scientific knowledge regarding changes in wind gusts and storminess from anemometer observations on multidecadal time scales is not conclusive. Table 1 reviews the few studies of long-term trends of wind speed extremes (not only DPWG) from anemometer observations for comparison purposes with the current study based on observations (listed #20 in Table 1). This shows that a majority of studies exhibit declining trends in wind speed extremes (11 studies; i.e., 55%), broadly in agreement with "stilling"; however, another 45% of studies reviewed report increasing or nontrending trends in wind speed extremes (see Table 1).

In view of (i) the minimal number of studies reporting long-term changes from observed DPWG over land; (ii) the overall inconclusive nature DPWG trends observed from anemometers; and (iii) the substantial societal and environmental impact of this natural hazard (e.g., for human safety, maritime and aviation activities, engineering and insurance applications, and energy production), additional trend assessments, and studies that assess these trends from a large-scale atmospheric circulation perspective are needed to increase our understanding of wind extremes [*Vose et al.*, 2014]. The principal objective of this study is to determine, for

Table 1. A Review of Long-Term Studies of Wind Speed Extremes (i.e., Not Only DPWG but Also, e.g., Maximum 1, 2, 10 min Wind Speed, Wind Speed in the Upper Tails, etc.) From Anemometer Observations[a]

Study #	Source	Data Details	Location	Period	Sign	Study Details: Magnitude of Trend or Finding
1	Klink [1999, Table 5]	187/10 m	U.S.	1961–1990	+	Overall increasing trend of $+0.037$ m s^{-1} decade^{-1}
2	Sweeney [2000, Table 3]	1/10 m	Dublin	1903–1999	-	Overall decreasing trend of -1.4 d^{-1} decade^{-1} for days with gusts >30 m s^{-1}
3	Pirazzoli and Tomasin [2003, Table 2]	17/10 m	Italy	1955–1996	–/+	-0.832 m s^{-1} decade^{-1} from 1951 to the mid-1970s; $+0.281$ m s^{-1} decade^{-1} from mid-1970s to mid-1990s
4	Alexander et al. [2005, Figure 3]	28/10 m	United Kingdom and Iceland	1950–2003	+/–	UK has seen a significant increase in the number of severe storms; fewer very severe events over Iceland.
5	Cabalar-Fuentes [2005, Table 3, Figures 2, and 3]	3/10 m	NW Spain	1961–2001	=/–	Nontrending change in the mean maximum wind speed; Storm events have decreased from ~5 to ~4 events a^{-1}, having shorter durations from ~5 to ~4 d event^{-1}
6	Smits et al. [2005, Figure 5]	13/10 m	The Netherlands	1962–2002	–	Storm events have decreased ~5–10% decade^{-1}
7	Mescherskaya et al. [2006, Table 1]	23/10 m	Russia	1936–2000	–	Decrease in stronger wind speed
8	Xu et al. [2006, Figure 1]	305/10 m	China	1969–2000	–	Prevalence of windy days (daily mean wind speed >5 m s^{-1}) has decreased by 58%
9	Fujii [2007, Section 7, p. 275]	150/various m	Japan	1966–2005	+	10 min mean wind speed greater than 20 m s^{-1} increased 1.5-fold from 1976–1985 to 1996–2005, and the incidence of wind speed greater than 35 m s^{-1} almost doubled over the same period.
10	Pryor et al. [2009, Figures 4–9]	2 data sets/10 m	U.S.	~1948–2006	–	In situ records depicted substantial decreases.
11	Jiang et al. [2010, Table 2]	535/10 m	China	1956–2004	–	-1.46 m s^{-1} decade^{-1} for maximum wind speed; -3.00 d^{-1} decade^{-1} for instantaneous and -0.79 d^{-1} decade^{-1} for sustained strong winds.
12	Kruger et al. [2010, Table 1]	4/10 m	South Africa	1993–2008	+	Average annual maximum wind gusts increased by $+0.09$ m s^{-1} decade^{-1}
13	Usbeck et al. [2010, Figure 6]	1/10 m	Canton Zurich, Switzerland	1891–2007	+	Increasing of maximum gust wind speed and severe winter storm damage in both amount and frequency since the 1960s.
14	Vautard et al. [2010, Figure 2]	822/10 m	Global, with a Northern Hemisphere focus	1979–2008	–	Strong winds have slowed faster than weak winds.
15	Hewston and Dorling [2011, Figures 4 and 5]	43/10 m	United Kingdom	1980–2005	–	-0.200 m s^{-1} decade^{-1} for observed daily maximum wind gusts.
16	Péliné Németh et al. [2011, Figures 3–7]	26/10 m	Hungary	1997–2010	–	Generally decreasing tendencies were found.
17	Cusack [2013, Figure 2]	5/10 m	The Netherlands	1910–2010	–	Downward trend in windstorm losses in the past two decades driven by reduced rate of occurrence of damaging storms.
18	Vose et al. [2014, Figure 3]	2 data sets/10 m	U.S.	~1973–2006	=	Evidence over land is inconclusive.
19	Klink [2015, Figures 3–5]	39/various m	U.S.	~1993–2009	+/–	Positive trends in the fastest 2 min wind speeds in winter, spring, and summer. Negative trends are most frequent in the autumn.
20*	Azorin-Molina et al. [2016, *Current study]	80/10 m	Spain and Portugal	~1961–2014	–	The annual frequency (-1.49 d decade^{-1}) and magnitude (-0.005 m s^{-1} decade^{-1}) of daily peak wind gusts have declined; however, a distinct seasonal/monthly trend pattern with declines in winter and increases in summer is found.

[a]The numbers provided in the data details represent the number of stations used in that study followed by the height of observations (in meters (m) above ground). The sign of trends is summarized as positive (+), negative (–), and nontrending (=). In the study details the magnitude of trend or the overall finding is reported. Studies are reported in increasing publication-date chronological order, then alphabetically within a year.

the first time, DPWG trends across the Iberian Peninsula (henceforth denoted by IP, covering Spain and Portugal). Our secondary objective focused on investigating the possible impact of the North Atlantic Oscillation index and the Jenkinson and Collison weather-typing classification on the observed variability of DPWG. Over this midlatitude region, the majority of extreme wind gust episodes are associated with extra-tropical cyclones during the cold season (November–April) [*Font-Tullot*, 2000] and with deep mesoscale thunderstorms (e.g., downbursts and rare tornadic activity) during the warm season (May–October) [*Azorin-Molina et al.*, 2015]. The complex topography of the IP also enhances the occurrence of severe damage wind events [*Ayala-Carcedo and Olcina-Cantos*, 2002], particularly in high mountainous summits and also on densely populated coastal areas [*Martin-Vide and Olcina-Cantos*, 2001].

2. Data, Homogenization, and Trend Analyses

2.1. Observed Daily Peak Wind Gusts

The World Meteorological Organization [*WMO*, 2008] (see chapter 5) defines gustiness as the turbulent fluctuations of wind speed. The observed DPWG data sets (in $m\,s^{-1}$), the highest single fluctuation of wind speed recorded in 24 h, were supplied by the Spanish Meteorological Agency (AEMET) and the Portuguese Sea and Atmosphere Institute (IPMA) and measured by anemograph and anemometer devices as reported [*Azorin-Molina et al.*, 2014]. The wind processing and recording systems of AEMET and IPMA comply with WMO requirements to compute daily extreme wind speed fluctuations, establishing the gust duration (i.e., measure of the duration of the observed peak gust) in ~3 s [*WMO*, 1987], from 0000 to 2400 h UTC.

The current availability of meteorological stations measuring DPWG is high across the IP: Spain (900 stations) and Portugal (16 stations). However, the length of most of these DPWG data series, particularly for Spain, is too short for trend analysis [*Weatherhead et al.*, 1998]. Therefore, stations were selected for use to provide a balance between (i) time series length, (ii) number of stations, and (iii) minimal disruptions due to relocation or replacement of traditional by new automatic weather stations. This selection resulted in 80 (73 for Spain and 7 for Portugal) long-term DPWG data series covering 54 years (1961–2014). All selected stations are first-order meteorological stations, i.e., well-exposed sites such as, e.g., airports, which ensure less immediate proximal environmental changes. All selected stations were subject to homogenization.

2.2. Homogenization of Daily Peak Wind Gusts

Taking into account the advantages of the robust homogenization proposed by *Azorin-Molina et al.* [2014], we used the Pennsylvania State University/National Center for Atmospheric Research mesoscale model MM5 [*Grell et al.*, 1994] to create reference series to homogenize the observed raw DPWG data set. Due to the ability of the MM5 to reproduce wind regimes and variability [e.g., *Pryor et al.*, 2009; *Jerez et al.*, 2012], these simulated series were used to detect and correct substantial mean shifts. Causes of break points in wind speed series have been extensively reported [*Pryor et al.*, 2009], with shifts produced by station relocations and/or anemometer height changes being particularly important [*Wan et al.*, 2010]. Hourly MM5 wind speed fields were retrieved at 10 m height at each station (i.e., interpolated from the nearest 10 km horizontal grid cells). As simulated, MM5 reference series were only available hourly; therefore, the simulated DPWG series were created taking the maximum hourly wind speed recorded in 24 h (from 0000 to 2400 h UTC). Even with this constraint, the histogram displayed in Figure 1 shows a good statistical agreement between the simulated and the observed DPWG series, with Pearson's correlation coefficients (*R*) dominating in the categories of *R* 0.6–0.7 (46.3%) and *R* 0.7–0.8 (36.3%). For a detailed description of the setup, configuration, and parameterization of the MM5 model [see *Jerez et al.*, 2013; *Azorin-Molina et al.*, 2014; *Lorente-Plazas et al.*, 2015].

Prior to initiating the homogenization against MM5 series, the observed raw DPWG series passed basic AEMET and IPMA quality controls to remove aberrant data due to digitalization [*Aguilar et al.*, 2003]. Moreover, we reconstructed observed DPWG series at 10 Spanish and 6 Portuguese stations that were relocated or replaced by automatic weather stations by concatenating the old and new series (the join dates were used to check for breaks). Once the observed DPWG data series passed the organizational quality control and reconstruction tasks, we applied the homogenization method implemented in the R package CLIMATOL version 2.2 (http://www.climatol.eu/, last accessed 1 November 2015), which uses the well-established relative Alexandersson's standard normal homogeneity test (SNHT) [*Alexandersson*, 1986] to detect sudden break points. This test is applied on differences between every single observed series and
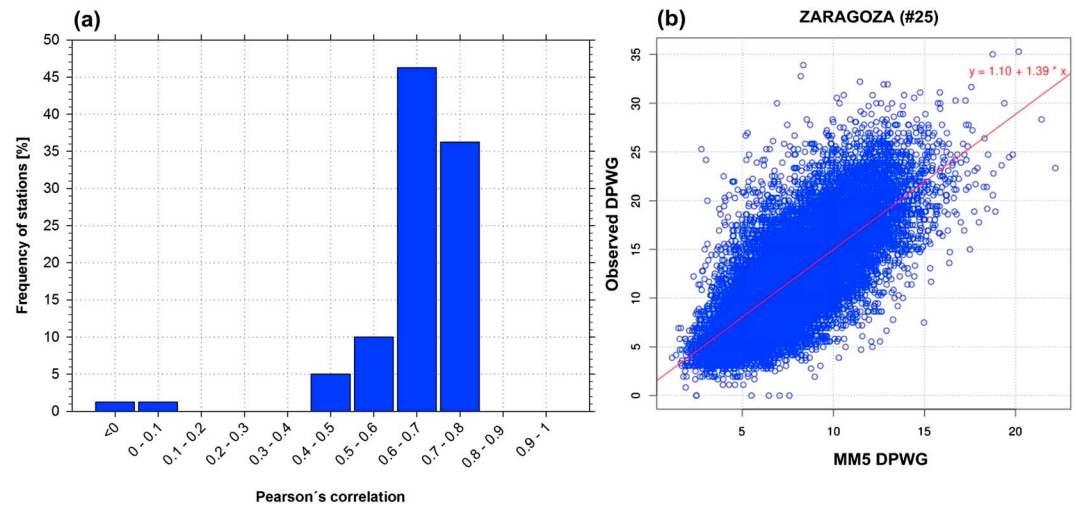
Figure 1. (a) Relative frequency histogram of the Pearson's correlation coefficients between the observed and simulated DPWG at the 80 homogenized stations; (b) scatterplot of observed versus simulated DPWG in Zaragoza (#25 in Table S1), with a residual standard error of 3.52 m s^{-1}, and R^2 of 0.52.

the simulated MM5 reference series, both in standardized form, in two ways (i) on stepped time windows to minimize the possible masking effects of multiple breaks and (ii) on the whole series. In each stage, series are successively split by the most significant break point in an iterative process until no SNHT value higher than a prescribed threshold remains, and all missing data are in filled using the standardized reference data at the end of the process. Our implemented homogenization procedure for wind speed data represents an improvement over previous versions of CLIMATOL achieved during the Committee on Science and Technology (COST) Action ES0601 and focused on homogenizing daily air temperature and precipitation series (advances in homogenization methods and integrated approach—HOME) [*Venema et al.*, 2012], and its skills are comparable to those of other good homogenization packages [*Guijarro*, 2011]. The homogenization of DPWG does not adopt the same steps applied by *Azorin-Molina et al.* [2014] and was performed directly on the daily series because a first exploratory homogenization of monthly aggregated values and further interpolation of monthly corrections to daily data did not yield good results. CLIMATOL provides a default threshold value of SNHT = 25 to split the series into two at the shift point. This is a conservative value compared to confidence limits found in the literature [e.g., *Khaliq and Ouarda*, 2007], to avoid errors in the process, but users may set their preferred limits. In fact, former experiences suggest that SNHT thresholds may be different depending on the variability of the series, which in turn is linked to the climatic element and time resolution analyzed. Therefore, users are advised to perform a first exploratory analysis with CLIMATOL and use the provided SNHT histograms to help choosing an appropriate value to discriminate inhomogeneous series. This is really the case when homogenizing daily values where, due to their lower noise/signal ratio, usual SNHT confidence limits would result in an exaggerated number of breaks. In this study, the exploratory analysis of the DPWG series moved us to choose SNHT thresholds of 150 and 500 for the overlapping windows and whole series applications, respectively.

Figure 2 provides four examples of the detection of noticeable breakpoints in the DPWG anomaly series by means of the SNHT test. To summarize, we detected and corrected 87 significant breaks, although two of them did not yield a homogeneous subperiod because of their small size and were just removed from their parent series. The effective 85 breaks corresponded to 53 series (31 series with 1 break, 13 series with 2 breaks, 8 series with 3 breaks, and 1 series with 4 breaks), and therefore, 27 out of the 80 series were found homogeneous. All 80 series were adjusted from their longest homogeneous subperiod for assessing long-term IP DPWG trends for 1961–2014. Figure 3 shows the location of the 80 homogenized stations across the IP, and the supporting information Table S1 describes their characteristics.

2.3. Atmospheric Circulation: NAOI and Jenkinson and Collison Scheme

With the secondary objective of assessing the influence of large-scale atmospheric circulation on the observed variability of DPWG, the North Atlantic Oscillation index (NAOI) and the automatic circulation-typing scheme of Jenkinson and Collison (JC) were chosen.
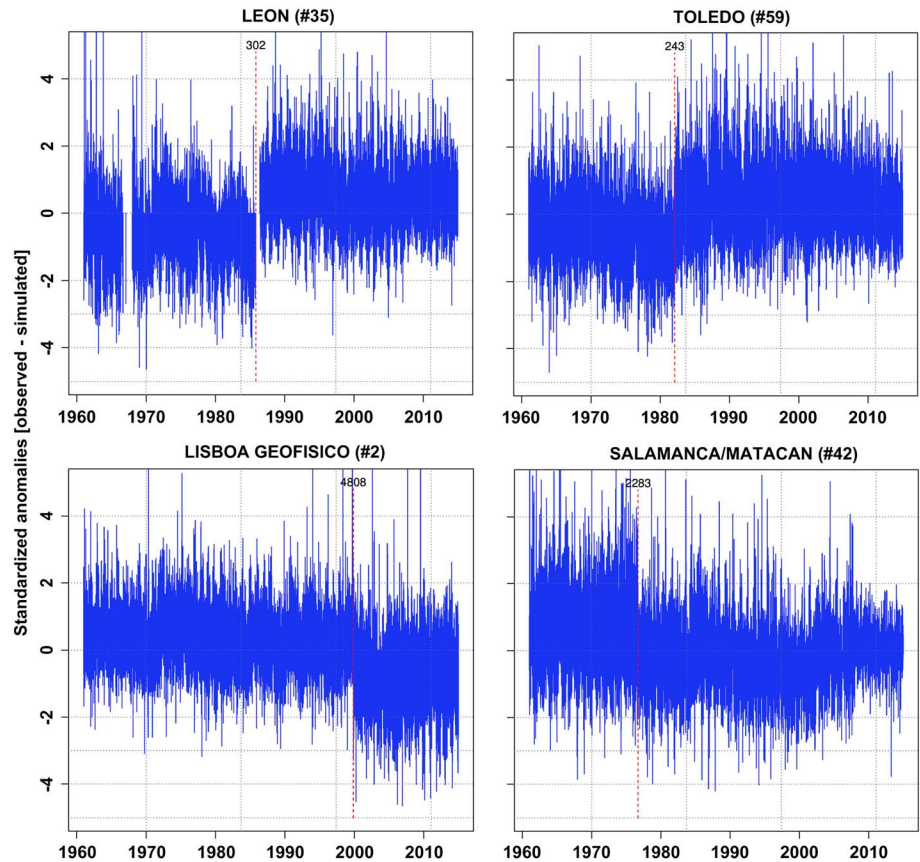
Figure 2. Examples of breakpoint detection (red dashed line with the SNHT value) by applying the SNHT test at four DPWG time series for 1961–2014. Numbers after the station names refer to the station number provided in Figure 3 and Table S1.

The NAOI drives much of the climate variability across the IP [e.g., *Vicente-Serrano and Trigo*, 2011, and the references therein] and partly the observed fluctuations in severe storms in Europe [e.g., *Ulbrich and Christoph*, 1999; *Alexander et al.*, 2005]. Here we used the NAOI defined by *Jones et al.* [1997] as the difference of normalized sea level pressure between Southwest IP (Gibraltar) and Southwest Iceland (Reykjavik) as
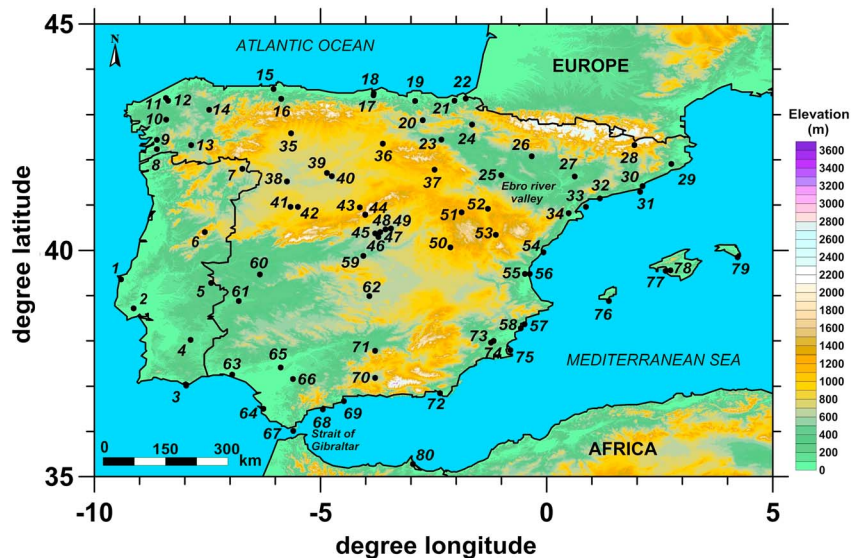

Figure 3. Terrain map of the IP showing the complex topography and location (for numbers see Table S1) of the 80 homogenized stations across the IP (except the Spanish station of Melilla—number 80, located in North Africa).

obtained from the Climatic Research Unit at http://www.cru.uea.ac.uk/cru/data/nao/ (last accessed 1 November 2015) using station-derived pressure series.

The JC scheme has been successfully applied as a "gale" indicator to study storminess in the UK [*Jenkinson and Collison*, 1977; *Donat et al.*, 2010] and more specifically to assess the relationship between climate variables and atmospheric circulation over the IP [e.g., *Azorin-Molina et al.*, 2011, and the references therein]. The JC method is based on objective rules concerning the calculation of seven equations or circulation indices. The objective rules compute the geostrophic wind and vorticity to determine the weather types (see below): equation (1) is the surface westerly component; equation (2) is the surface southerly component; equation (3) is the computation of the surface geostrophic wind; equation (4) is the wind direction; equation (5) is the westerly vorticity; equation (6) is the southerly vorticity; and equation (7) is the total vorticity (for details see *Azorin-Molina et al.* [2011]). The synoptic catalog identifies 27 weather types grouped into four categories (i) directional flow types (N, NE, E, SE, S, SW, W, and NW); (ii) anticyclonic (A) and cyclonic (C) types related to the rotation of the atmosphere; (iii) hybrid types (AN, ANE, AE, ASE, AS, ASW, AW, ANW, CN, CNE, CE, CSE, CS, CSW, CW, and CNW); and (iv) the unclassified type (UD). We extended the original grid basis of *Spellman* [2000] to classify the UD type, and therefore, 26 weather types were used here.

2.4. Trend Analysis

We analyzed the spatiotemporal trends of two peak wind gust parameters (i) the frequency of DPWG exceeding the 90th percentile of the entire 19,723 days (54 years from 1961 to 2014) population at each station and (ii) the magnitude (maximum wind speed) of DPWG. Therefore, the 80 single homogenized DPWG data series were converted into two series. First, when in the series the days in the highest DPWG decile, i.e., those exceeding the 90th percentile [*Vose et al.*, 2014], were determined at each station on an annual, seasonal and monthly basis independently. For instance, we found the 90th percentile of DPWG for all summers for 1961–2014 and then count the number of summer days in each year exceeding this percentile. Second, daily wind speed maxima data were averaged to annual, seasonal and monthly mean DPWG (in $m\,s^{-1}$) for each station. We analyzed long-term trends of the frequency and magnitude of DPWG at annual, seasonal, and monthly time steps for each station and averaged for three regional series comprised of (i) 80 (All IP), (ii) 73 (Spain), and (iii) 7 (Portugal) stations. Seasonal statistics comprises the following months: winter (December–February (DJF)), spring (March–May (MAM)), summer (June–August (JJA)), and autumn (September–November (SON)).

The sign and magnitude of changes in the frequency and magnitude of DPWG for 54 years (1961–2014) are expressed in days per decade ($d\,decade^{-1}$) and meters per second per decade ($m\,s^{-1}\,decade^{-1}$), respectively. This is achieved by performing linear regression analysis to calculate the slope between the series of time (independent variable or X axis) and at annual, seasonal, and monthly time steps (i) the number of days in the highest decile and (ii) wind speed maxima (in turn, as the dependent variable or Y axis). Additionally, a 15 years Gaussian low-pass filter to highlight decadal variability was plotted. To quantify the degree of change of long-term trends of the frequency and magnitude of DPWG, a multistep statistical approach was employed consisting of (i) 1 month lag autocorrelation coefficient [*von Storch*, 1995] since significant autocorrelations may increase the probability of detecting a statistically significant trend, (ii) applying the nonparametric correlation coefficient of Mann-Kendall's tau-b [*Kendall and Gibbons*, 1990] to report the statistical significance of the linear trends by, (iii) expressing significant trends at three p level thresholds (significant at $p < 0.05$, significant at $p < 0.10$, and not significant at $p < 0.10$) as suggested by *McVicar et al.* [2010] to consider trends from a "process and importance" perspective, and (iv) to evaluate field significance (at the three abovementioned confidence levels) of the significant trends [*Livezey and Chen*, 1983; *Wilks*, 2006] in order to detect whether the number of stations with significant trends have occurred by chance [*Dadaser-Celik and Cengiz*, 2014]. Lastly, at annual, seasonal and monthly time scales the impact of NAOI and JC weather types on the temporal variability of the mean number of DPWG exceeding the 90th percentile (frequency) and the mean DPWG (magnitude) for the three regional series, was measured by the Pearson's correlation coefficient (R).

3. Results

Sections 3.1 to 3.3 address our primary objective of assessing DPWG trends across the IP, and sections 3.4 and 3.5 relate to our secondary objective of quantifying the impact of large-scale atmospheric circulation (NAO and JC weather types) on the observed DPWG trends.
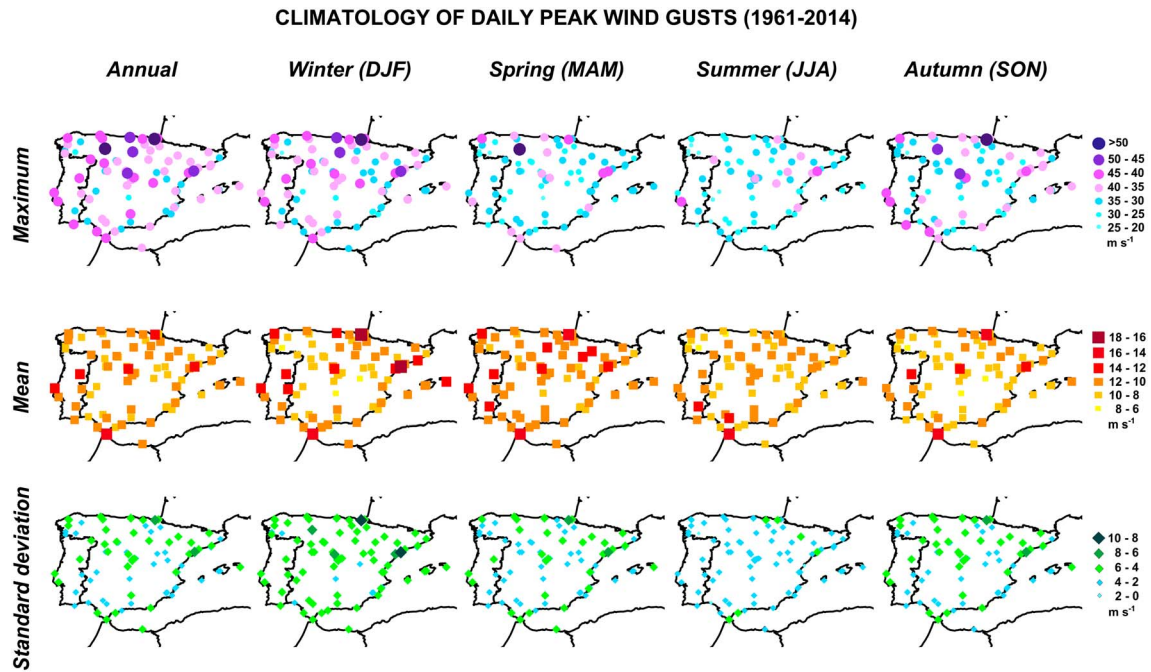
CLIMATOLOGY OF DAILY PEAK WIND GUSTS (1961-2014)

Figure 4. Annual and seasonal spatial distribution of the maximum, mean, and standard deviation (in m s^{-1}) of DPWG for all 80 homogenized stations for 1961–2014.

3.1. Climatology of DPWG

The spatial climatology of the homogenized DPWG data set across the IP is shown in Figure 4 by reporting three statistical parameters (i.e., maximum, mean, and standard deviation) for each of the 80 stations at annual and seasonal scales during 1961–2014. Additionally, box-and-whisker plots shown in Figure 5 summarize the intra-annual variation of DPWG (supporting information Figure S1 shows monthly plots). Annually, maximum DPWG have primarily been recorded over the northwestern and western IP, i.e., those areas which are more exposed to Atlantic extratropical cyclones with strong winds. Over this region, the highest DPWG was measured in San Sebastian (station number 21) at 51.9 m s^{-1}, followed by 51.5 m s^{-1} in Leon (station number 35), and 46.4 m s^{-1} in Santander (station number 17). There are other isolated regions showing extreme DPWG, such as the mountainous Navacerrada station (station number 44; 49.4 m s^{-1}) in the Central System range, or the Vandellos station (station number 33; 45.8 m s^{-1}) located at the mouth of the Ebro river valley in the Mediterranean, i.e., where northwesterly winds are channeled. In Portugal (i.e., western IP), the highest DPWG was measured in Faro (station number 3) with 43.7 m s^{-1}. The areas where maximum DPWG are small correspond to some inland stations or locations with particular topographic features (e.g., leeward side of prevailing winds) that weaken extreme winds: e.g., Ciudad Real (station number 62) 28.9 m s^{-1}, Murcia (station number 73) 28.6 m s^{-1}, and Ourense (station number 13) 25 m s^{-1}. Figure 4 (top row) shows that seasonally the spatial distribution of maximum DPWG resembles the annual analysis for winter, spring, and autumn, whereas in summer this maximum DPWG is primarily located in eastern IP.
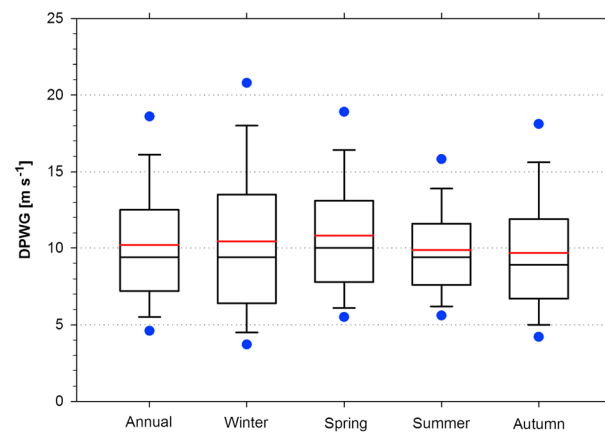

Figure 5. Annual and seasonal box-and-whisker plots of DPWG for all 80 homogenized series for 1961–2014. The mean (red line), the median (black line), the 25th and 75th percentile range (boxes), the 10th and 90th percentiles (whiskers), and the 5th and 95th percentiles (blue dots) are represented. Monthly box-and-whisker plots are shown in the supporting information Figure S1.

Table 2. Annual and Seasonal Trends in the Mean Frequency of DPWG Exceeding the 90th Percentile (d decade^{-1}) and Mean Magnitude DPWG (m s^{-1} decade^{-1}) for All 80 Stations, Spain (73 Stations) and Portugal (7 Stations) for 1961–2014[a]

	Mean Frequency DPWG Trends (d decade^{-1})			Mean Magnitude DPWG Trends (m s^{-1} decade^{-1})		
Periods	All stations	Spain	Portugal	All stations	Spain	Portugal
Annual	(**−1.49**)	(**−1.55**)	−0.79	−0.005	0.003	(**−0.091**)
Winter (DJF)	(**−0.73**)	(**−0.76**)	−0.40	**−0.168**	**−0.168**	**−0.168**
Spring (MAM)	(**−0.50**)	(**−0.52**)	−0.24	−0.015	−0.008	(**−0.092**)
Summer (JJA)	0.18	**0.20**	−0.13	(**0.130**)	(**0.148**)	−0.045
Autumn (SON)	−0.39	(**−0.43**)	0.03	0.035	0.041	−0.040

[a]Statistically significant trends were defined as those $p < 0.10$ (in bold) and $p < 0.05$ (in bold and in parenthesis).

According to the climatology (Figure 4) and the box-and-whisker plots (Figure 5 and supporting information Figure S1 for monthly plots), winter registered the strongest wind extreme episodes, followed by spring and autumn, with summer being the season when maximum wind gust events were weakest.

When looking at the mean DPWG (Figure 4, middle row) some interesting features are found. Overall, mean annual DPWG is 10.2 m s^{-1}, with spring (10.8 m s^{-1}) the windiest season, followed by winter (10.4 m s^{-1}), summer (9.9 m s^{-1}), and autumn (9.7 m s^{-1}). Spatially, the areas where high mean DPWG is observed are very similar to the maximum maps (Figure 4, top row). Annually, the highest mean DPWG is recorded in Tarifa (Strait of Gibraltar; station number 67) with 14.7 m s^{-1} due to the channeling of westerlies/easterlies in all seasons. Other areas of high mean DPWG are coincidental to where maximum wind extremes were recorded: i.e., San Sebastian 13.9 m s^{-1} (Bay of Biscay), Vandellos 13.4 m s^{-1} (mouth of the Ebro river valley), and mountainous stations such as Navacerrada and Penhas Doradas (station number 6) with 12.4 m s^{-1}. In contrast, the lowest mean DPWG values were registered in Ciudad Real with 7.9 m s^{-1} and Ourense with 7.6 m s^{-1}, both inland stations protected against synoptic winds and/or with weak local wind circulations.

Lastly, the spatiotemporal variability of DPWG is illustrated by the standard deviations (Figure 4, bottom row), and the interquartile range (25th and 75th percentiles) shown in the box-and-whisker plots (Figure 5 and supporting information Figure S1 for monthly plots). Winter displays the highest interquartile range (7.0 m s^{-1}), denoting the high variability of DPWG because of the switching between strong winds and anticyclonic calm conditions [Font-Tullot, 2000; Martin-Vide and Olcina-Cantos, 2001]. Spring and autumn show a moderate interquartile range (5.3 m s^{-1}), whereas summer presents the lowest range (3.9 m s^{-1}). These seasonal differences are clearly seen in the standard deviation analysis (Figure 4, bottom row), where Vandellos (7.5 m s^{-1}) and San Sebastian (7.2 m s^{-1}) are the two stations with the highest standard deviations annually and seasonally.

A particular feature of DPWG statistics shown in Figure 4, 5 and supplementary Figure S1 is that seasons/months with the highest DPWG (e.g., winter) do not correspond to the seasons/months with the highest average of DPWG (e.g., spring); this is because the frequency and intensity of weather patterns associated with strong wind gusts (e.g., westerly winds) vary throughout the year.

3.2. Long-Term Spatiotemporal Trends in the Frequency of Extreme DPWG

Table 2 summarizes annual and seasonal trends of the mean number of days exceeding the 90th percentile of DPWG for all stations for 1961–2014. Annually, we found a statistically significant (at $p < 0.05$) declining trend in the occurrence of extreme wind gusts, with a reduction of −1.49 d decade^{-1} averaged across all 80 stations. Seasonally, this decreasing trend in the frequency of DPWG was prominent in winter, spring, and autumn, whereas an increasing trend was encountered in summer. For instance, the strongest downward trend of extreme wind gust episodes occurred in winter with −0.73 d decade^{-1} (significant at $p < 0.05$), followed by spring with −0.50 d decade^{-1} (significant at $p < 0.05$), and autumn with −0.39 d decade^{-1} (significant at $p < 0.10$). In contrast, we found a slightly increase (but not statistically significant at $p < 0.10$) in the frequency of DPWG in summer of +0.18 d decade^{-1} (Table 2).

Figure 6 displays annual and seasonal temporal variability of the mean number of days exceeding the 90th percentile recorded over 19,723 days (54 years from 1961 to 2014) averaged over the Spanish (73 stations) and Portuguese (7 stations) series separately. Note that both regional series present similar temporal variability as shown by the 15 years Gaussian low-pass filter, displaying a strong consistency by being
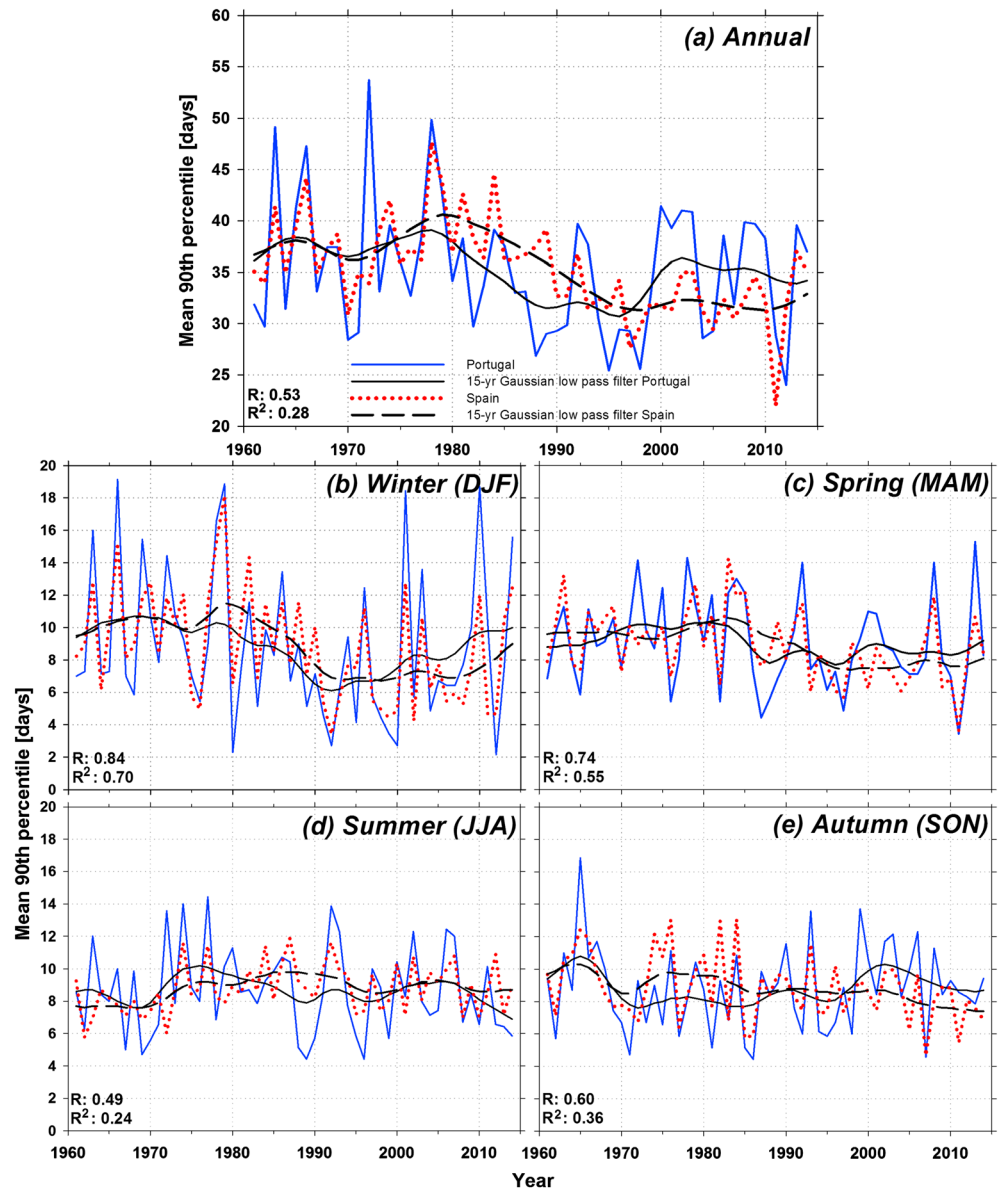
Figure 6. Mean annual and seasonal number of days exceeding the 54 year 90th percentile for Spain (red dotted line) and Portugal (blue solid line) from 1961 to 2014. The 15 years Gaussian low-pass filter is also shown with a black dashed line for Spain and with a black solid line for Portugal. Monthly plots are shown in the supporting information Figure S2. The Pearson's correlation coefficient (R) and the coefficient of determination (R^2) are also reported.

significantly (at $p < 0.05$) correlated with R values of 0.53 annually (Figure 6a), 0.84 in winter (Figure 6b), 0.74 in spring (Figure 6c), 0.49 in summer (Figure 6d), and 0.60 in autumn (Figure 6e); confirming the robustness and quality of the daily homogenization performed on the raw DPWG data sets provided by the two National Weather Services. Annually, the declining trend in the frequency of extreme DPWG events (i.e., the highest 10% of observed winds in the entire 54 year population) is ~2 times higher in magnitude for Spain (-1.55 d decade^{-1}; significant at $p < 0.05$) than for Portugal (-0.79 d decade^{-1}; not significant at $p < 0.10$). Long-term variability shown by the 15 years Gaussian low-pass filters can be divided into three trend periods (i) weak increase from 1961 to 1980; (ii) pronounced decline from 1980 to 1998; and (iii) slight increase of the occurrence of DPWG episodes from 1998 to 2014. Seasonally, Spain showed the abovementioned long-term trend pattern with decreasing tendencies in winter (-0.76 d decade^{-1}; significant at $p < 0.05$), spring (-0.52 d decade^{-1}; significant at $p < 0.05$), and autumn (-0.43 d decade^{-1}; significant at $p < 0.05$), and increasing in summer ($+0.20$ d decade^{-1}; significant at $p < 0.10$) over the 54 year record. Portugal also
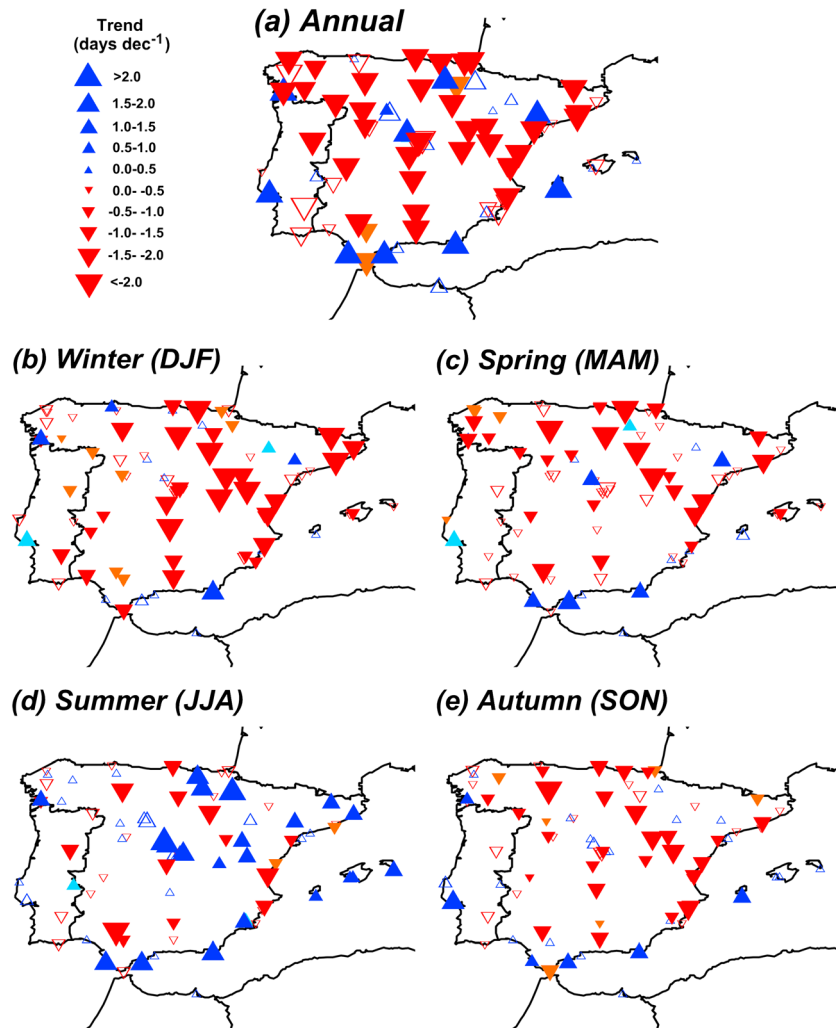
Figure 7. Spatial distribution of the sign, magnitude of trend (d decade^{-1}), and significance (blue and red filled triangles are significant at $p < 0.05$; light blue and orange filled triangles are significant at $p < 0.10$; and nonfilled triangles are not significant at $p < 0.10$) of annual and seasonal number of days exceeding the 54 year 90th DPWG percentile trends for 80 stations for 1961–2014.

displayed declining trends in winter (-0.40 d decade^{-1}), spring (-0.24 d decade^{-1}), and also in summer (-0.13 d decade^{-1}), whereas a very weak increasing trend was observed in autumn ($+0.03$ d decade^{-1}); all these trends were not being statistically significant at $p < 0.10$. The supporting information Figure S2 and Table S2 show the monthly long-term trends in the frequency of extreme DPWG.

The spatial distribution of the 80 station-based trends (i.e., sign, magnitude of change, and statistical significance) is shown in Figure 7 and summarized in Table 3a. Annually (Figure 7a), there is a clear dominance of declining trends (71.3% of stations; with 59.6% being significant at $p < 0.05$) in the frequency of extreme wind gusts exceeding the 90th percentile over the entire 54 year population. Seasonally, this decreasing trend pattern also dominates, particularly in winter (80.0%; 46.9% significant at $p < 0.05$, Figure 7b) and spring (81.3%; 40.0% significant at $p < 0.05$, Figure 7c), with the percentages being slightly lower in autumn (67.5%; 50.0% significant at $p < 0.05$, Figure 7e). It is noteworthy to highlight that the strongest declining trends are located in windy areas, such as, e.g., the Cantabrian coast, and particularly the Ebro river valley (e.g., in spring, the windiest season there), or the Mediterranean coast. The exception to this widespread declining pattern occurs in summer (Figure 7d) with the majority of stations showing increasing trends (53.8%; 48.8% significant at $p < 0.05$); these are located along the Mediterranean coast, some inland stations,

Table 3. Relative Percentage of Stations With Significant (at $p < 0.05$ and $p < 0.10$) and Nonsignificant (at $p < 0.10$) Negative and Positive Trends in (a) the 90th Percentile of DPWG and (b) Magnitude of DPWG Annually and Seasonally for 1961–2014 for 80 Stations Across the IP[a]

	Negative	Negative $p < 0.05$	Negative $p < 0.10$	Negative $p > 0.10$	Positive	Positive $p < 0.05$	Positive $p < 0.10$	Positive $p > 0.10$
				(a) Frequency				
Annual	71.2	59.6	64.9	35.1	28.8	43.5	47.8	52.2
Winter (DJF)	80.0	46.9	59.4	40.6	20.0	25.0	37.5	62.5
Spring (MAM)	81.2	40.0	46.2	53.8	18.8	33.3	46.7	53.3
Summer (JJA)	46.2	35.1	43.2	56.8	53.8	48.8	53.5	46.5
Autumn (SON)	67.5	50.0	61.1	38.9	32.5	23.1	23.1	76.9
				(b) Magnitude				
Annual	47.5	42.1	13.2	44.7	52.5	28.6	7.1	64.3
Winter (DJF)	83.8	43.3	7.5	49.3	16.3	7.7	15.4	76.9
Spring (MAM)	53.8	32.6	4.7	62.8	46.3	24.3	8.1	67.6
Summer (JJA)	18.8	33.3	6.7	60.0	81.3	63.1	0.0	36.9
Autumn (SON)	37.5	40.0	3.3	56.7	62.5	26.0	14.0	60.0

[a]For the three p level thresholds, relative frequencies are calculated with respect to the total number of stations showing negative or positive tendencies. Spatial distributions are shown in Figure 7 for frequency trends and Figure 10 for magnitude trends.

and the Cantabrian coast (Bay of Biscay). This intra-annual pattern is clearly discernible in the monthly maps shown in Figure 8, and the statistical summary provided in the supporting information Table S3a.

3.3. Long-Term Spatiotemporal Trends in the Magnitude of DPWG

Annually, while we observed a statistically significant decline in the frequency of extreme wind gusts, the magnitude of the DPWG trend was small ($-0.005 \, \mathrm{m\,s^{-1}\,decade^{-1}}$; not significant at $p < 0.10$) for all 80 stations during 1961–2014 (Table 2). Seasonally, the significant tendency of decreasing frequency of extreme wind gust episodes in winter was accompanied by a decline in its magnitude ($-0.168 \, \mathrm{m\,s^{-1}\,decade^{-1}}$; significant at $p < 0.10$). However, we found that the significant decreasing trend in the frequency of DPWG in spring and autumn is not associated with a significant loss of their magnitude; e.g., the mean velocity of DPWG only slightly decreased in spring ($-0.015 \, \mathrm{m\,s^{-1}\,decade^{-1}}$; not significant at $p < 0.10$) and on the contrary weakly increased in autumn ($+0.035 \, \mathrm{m\,s^{-1}\,decade^{-1}}$; not significant at $p < 0.10$). For this latter season,
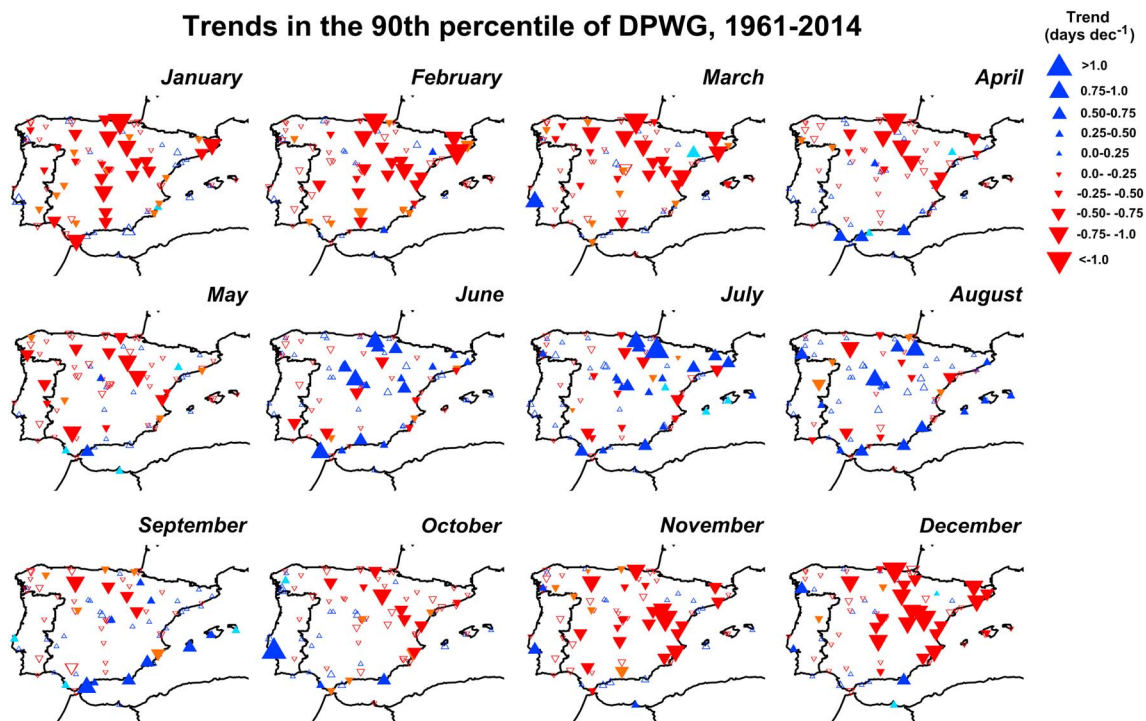

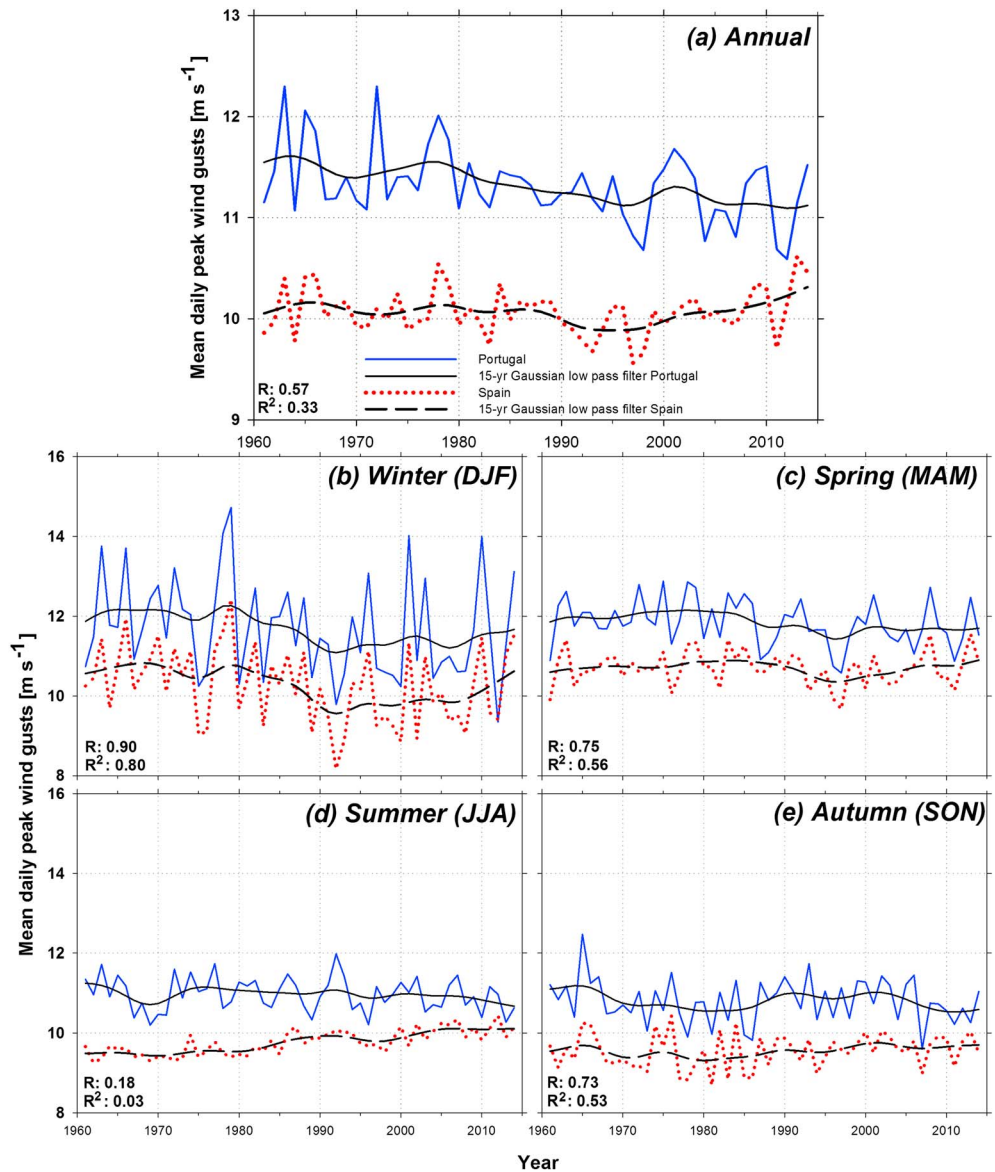**Figure 8.** As in Figure 7, but for monthly plots.

Figure 9. Annual and seasonal mean wind speed of DPWG for Spain (red dotted line) and Portugal (blue solid line) from 1961 to 2014. The 15 years Gaussian low-pass filter is also shown with a black dashed line for Spain and with a black solid line for Portugal. Monthly plots are shown in the supporting information Figure S3. The Pearson's correlation coefficient (R) and the coefficient of determination (R^2) are also reported.

this means less frequent but higher magnitude DPWG events. Lastly, the increasing trend in the frequency of DPWG in summer was accompanied by a significant increase in the magnitude of extreme wind gust episodes (+0.130 m s^{-1} decade^{-1}; significant at $p < 0.05$).

The annual and seasonal variability in the magnitude of DPWG over the Spanish (73 stations) and Portuguese (7 stations) series for 1961–2014 is shown in Figure 9. As the frequency series displayed in Figure 6, both regional series show, except for summer, a statistically significant (at $p < 0.05$) relationship with R values of 0.57 annually (Figure 9a), 0.90 in winter (Figure 9b), 0.75 in spring (Figure 9c), 0.18 in summer (Figure 9d), and 0.73 in autumn (Figure 9e). Annually, while the Portuguese series (average for 7 stations) showed a declining trend in the magnitude (−0.091 m s^{-1} decade^{-1}; significant at $p < 0.05$) in accordance with the negative trend detected in the frequency of extreme wind gusts, we found no trend (albeit only a slightly positive of +0.003 m s^{-1} decade^{-1}; not significant at $p < 0.10$) in the magnitude of DPWG for the Spanish series (average for 73 stations), which contrasts with the significant negative tendency in the frequency of extreme
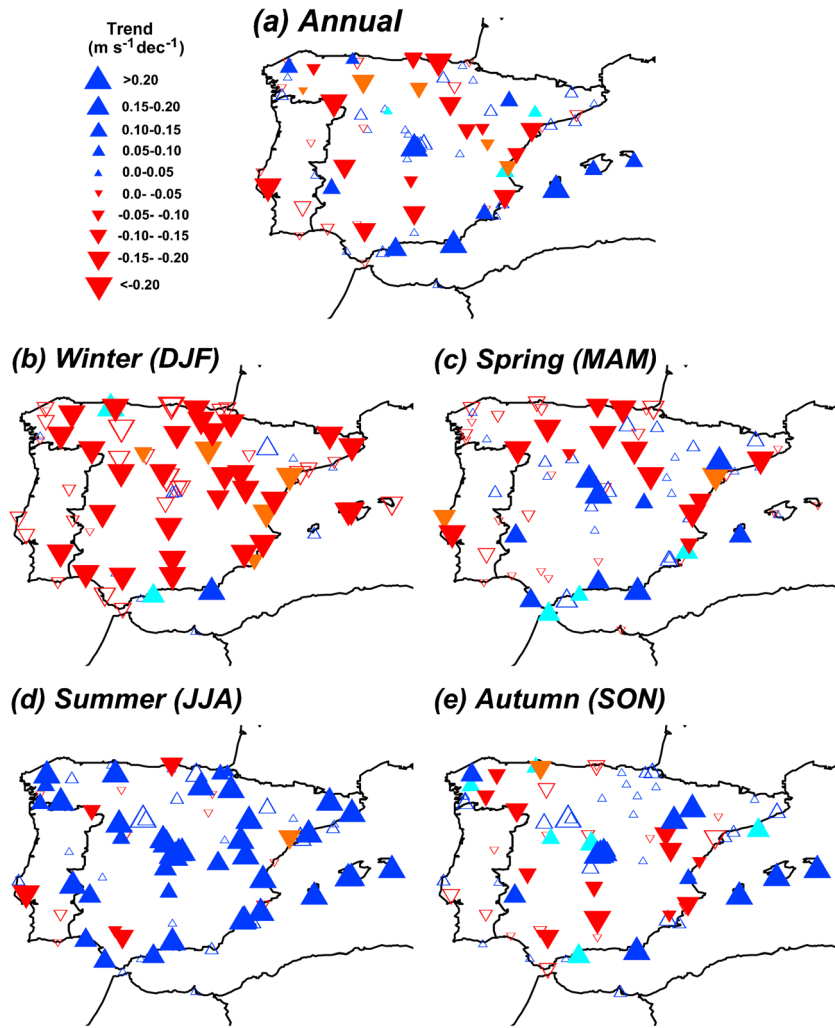
Trends in the mean of DPWG, 1961-2014

Figure 10. Spatial distribution of the sign, magnitude of trend (d decade^{-1}), and significance (blue and red filled triangles are significant at $p < 0.05$; light blue and orange filled triangles are significant at $p < 0.10$; and nonfilled triangles are not significant at $p < 0.10$) of trends in annual and seasonal mean DPWG for 80 stations for 1961–2014.

wind events. More specifically, this resultant weakening long-term trend is due to the increase in the magnitude (and frequency) of wind gusts observed since ~1998. Seasonally, winter exhibited an overall and equal decline in the magnitude of DPWG for both the Spanish and Portuguese 54 year series (-0.168 m s^{-1} decade^{-1}; significant at $p < 0.10$), even though increases were observed in the last decade. In spring, no trend or weakly negative was detected in Spain (-0.008 m s^{-1} decade^{-1}; not significant at $p < 0.10$), whereas Portugal showed a decline in magnitude of wind extreme events (-0.092 m s^{-1} decade^{-1}; significant at $p < 0.05$). For the remaining seasons (i.e., autumn and summer), Spain showed increases of the magnitude of DPWG events, particularly in summer ($+0.148$ m s^{-1} decade^{-1}; significant at $p < 0.05$) and with lesser statistically significance in autumn ($+0.041$ m s^{-1} decade^{-1}; not significant at $p < 0.10$); while Portugal displayed decreasing trends in summer (-0.045 m s^{-1} decade^{-1}) and autumn (-0.040 m s^{-1} decade^{-1}), neither significant at $p < 0.10$. The supporting information Figure S3 and Table S2 show the monthly long-term trends in the magnitude of DPWG, essentially replicating these seasonal findings with greater temporal granularity.

In Figure 10 and Table 3b the annual and seasonal spatial distribution and relative frequency statistics, respectively, of the 80 station-based trends of the mean of DPWG (magnitude) are provided. Annually (Figure 10a), there is not a consistent trend detected, with near half of the stations each showing decreasing
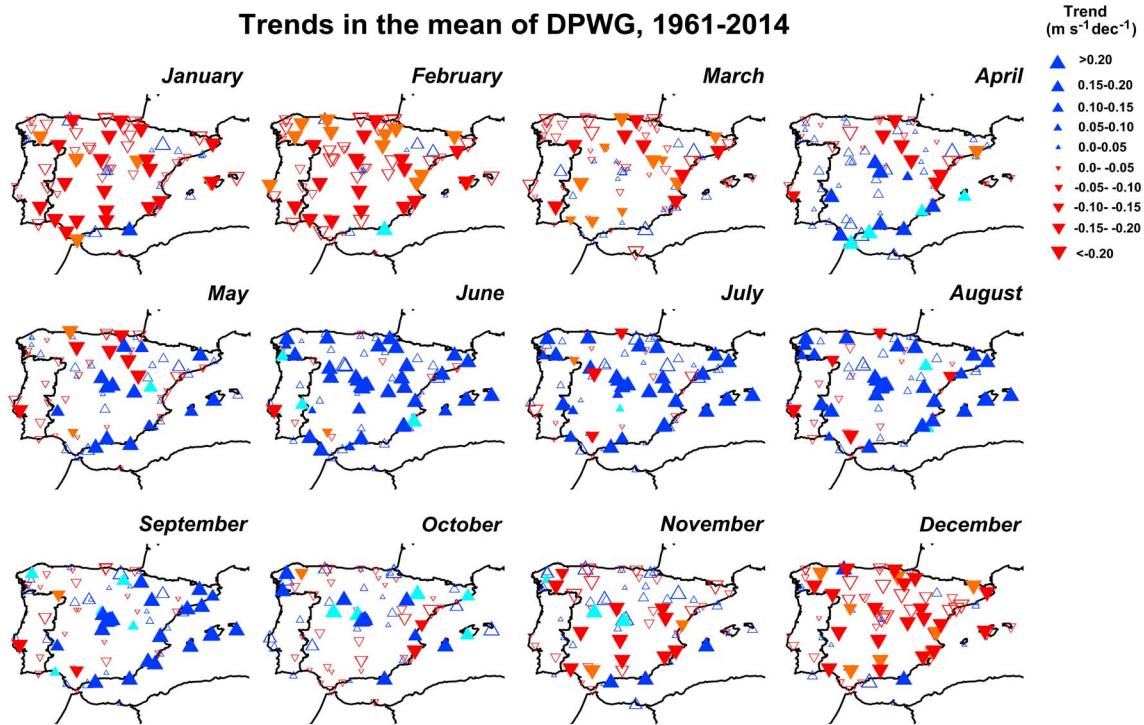
Figure 11. As in Figure 10, but for monthly plots.

(47.5%; being 42.1% significant at $p < 0.05$) and increasing (52.5%; being 28.6% significant at $p < 0.05$) trends. Seasonally, the magnitude of DPWG markedly declined for a high percentage of stations in winter (83.8%; being 43.3% significant at $p < 0.05$; Figure 10b), which means, according to the trends in the 90th percentile, less frequent and lower magnitude DPWG across the IP. In spring (Figure 10c), there was a reduction of these negative trends (53.8%; being 32.6% significant at $p < 0.05$), mostly occurring over the northern and eastern IP (e.g., Cantabrian coast, the Ebro river valley, and the Mediterranean coast), whereas positive trends (46.2%; being 24.3% significant at $p < 0.05$) dominated across the southern IP. Moreover, the increasing trend in the frequency of DPWG is also detected in the magnitude of wind gusts in summer (Figure 10d), with a significant dominance of positive trends (81.3%; being 63.1% significant at $p < 0.05$). Lastly, no clear pattern was detected in autumn (Figure 10e), even though positive trends in the magnitude of DPWG dominated (62.5%; being 26.0% significant at $p < 0.05$). This seasonal pattern is markedly reinforced in the monthly maps and statistics shown in the supplementary Figure 11 and Table S3b, respectively, where negative trends in the magnitude of DPWG dominated from November to April and positive trends from May to October are seen.

3.4. The North Atlantic Oscillation

Annual and seasonal Pearson's correlation coefficients (R) shown in Table 4 (monthly statistics are provided in Table S4) indicate that the NAOI exerted its major influence on the decadal variability of DPWG in winter. This

Table 4. Annual and Seasonal Trends of NAOI (Values Are Expressed as Standardized Sea Level Pressure Difference) and for All 80 Stations Across Spain and Portugal for 1961–2014 the Pearson's Correlation Coefficients Between: (i) the Mean Number of DPWG Exceeding the 90th Percentile and NAOI and (ii) the Mean Magnitude DPWG and NAOI[a]

Periods	NAOI	Mean Frequency DPWG (R-Pearson)			Mean Magnitude DPWG (R-Pearson)		
		All stations	Spain	Portugal	All stations	Spain	Portugal
Annual	−0.065	0.07	0.08	−0.09	**−0.22**	**−0.23**	−0.10
Winter (DJF)	0.146	(**−0.47**)	(**−0.45**)	(**−0.56**)	(**−0.55**)	(**−0.53**)	(**−0.61**)
Spring (MAM)	−0.032	−0.16	−0.15	**0.27**	−0.17	−0.18	−0.06
Summer (JJA)	(**−0.197**)	−0.13	−0.12	−0.12	(**−0.33**)	(**−0.33**)	−0.12
Autumn (SON)	(**−0.194**)	−0.06	−0.03	**0.26**	(**−0.32**)	(**−0.31**)	(**−0.33**)

[a]Statistically significant correlations were defined as those $p < 0.10$ (in bold) and $p < 0.05$ (in bold and in parenthesis).

Table 5. Most Positive and Negative Annual and Seasonal Pearson's Correlation Coefficients (R) and the Corresponding Jenkinson and Collison (JC) Regime for the Relationship Between the Mean Number of DPWG Exceeding the 90th Percentile and the Frequency Series of 26 Jenkinson and Collison Weather Types for All Stations for 1961–2014[a]

Periods	Mean Frequency DPWG				Mean Magnitude DPWG			
	JC	+ R	JC	− R	JC	+ R	JC	− R
Annual	W	**(0.49)**	CE	−0.25	W	**(0.50)**	ASE	**(−0.41)**
Winter (DJF)	W	**(0.57)**	A	**(−0.40)**	W	**(0.59)**	ASE	**(−0.45)**
Spring (MAM)	W	**(0.59)**	SE	**(−0.40)**	N	**(0.54)**	SE	**(−0.38)**
Summer (JJA)	W	**(0.35)**	E	−0.17	NW	**0.25**	N	**−0.26**
Autumn (SON)	N	**(0.39)**	E	**(−0.48)**	W	**(0.49)**	S	**(−0.43)**

[a]The same for the mean magnitude DPWG. Significant correlations were defined as those $p < 0.10$ (in bold) and $p < 0.05$ (in bold and in parenthesis).

statistically significant relationship ($p < 0.05$) is negative for the mean number of DPWG exceeding the 90th percentile (R of −0.47 for all stations, −0.45 for Spain, and −0.56 for Portugal), being a bit greater for the mean magnitude DPWG (R of −0.55 for all stations, −0.53 for Spain, and −0.61 for Portugal). These show that negative phases of the NAOI, linked to the formation (and/or passing) of low-pressure systems over the IP and a strong blocking anticyclone in the North Atlantic region, drive large-sale synoptic winds and, therefore, has a strong influence on DPWG characteristics. The slightly higher R values found between NAOI and mean magnitude DPWG, when compared to that between NAOI and the mean number of DPWG exceeding the 90th percentile, is because mean daily wind gusts better represent the influence of atmospheric dynamics when only looking at the highest magnitude wind gust episodes. This is clearly discernible for the remaining time scales, i.e., annual, spring, summer, and autumn. For instance, whereas the relationship between NAOI and the mean number of DPWG exceeding the 90th percentile is very weak, with the exception of a statistically significant relationship ($p < 0.10$) for Portugal in spring (R of −0.27) and autumn (R of −0.26), the mean magnitude DPWG shows a stronger influence of this atmospheric teleconnection pattern. Annually, statistically significant relationships ($p < 0.10$) are found for all stations (R of −0.22) and Spain (R of −0.23), becoming significant at $p < 0.05$ in summer (R of −0.33 for all stations and Spain) and autumn (R of −0.32 for all stations, −0.31 for Spain, and −0.33 for Portugal). The NAOI influence on variability of DPWG in spring is weakly negative but not statistically significant ($p < 0.10$). When assessing the long-term trends of this large-scale circulation mode (see Table 4; monthly statistics in Table S4), we found a positive but not significant ($p < 0.10$) decadal trend of the winter NAOI (+0.146), which might be driving the less frequent and intense DPWG observed across the IP. In contrast, negative and statistically significant ($p < 0.05$) trends of summer (−0.197) and autumn (−0.194) NAOI might partly explain the more frequent and higher magnitude DPWG detected in both these seasons.

3.5. Jenkinson and Collison Weather Types

As summarized in Table 5, annually, both the frequency and magnitude of DPWG, respectively, show the highest positive statistically significant relationship (i.e., weather types enhancing more frequent and intense wind gusts) for the W regime (R 0.49 and 0.50, $p < 0.05$), whereas the most negative R (i.e., weather patterns inhibiting wind gusts) occurred for the CE (−0.25; $p < 0.10$) and ASE (−0.41; $p < 0.05$) synoptic patterns. Seasonally, the W type also shows the highest positive significant relationship in winter (R 0.57 and 0.59; $p < 0.05$), whereas the lowest correlation is found for the A and ASE synoptic types. In spring, the highest positive and statistically significant relationships differ between the frequency of DPWG where the W type still dominating (R 0.59; $p < 0.05$) and the magnitude of DPWG with the N regime (R 0.54; $p < 0.05$) driving wind gust variability; in contrast, the most negative correlation coefficients are found for the SE type. In summer, the frequency and magnitude of DPWG is positively linked to the W (R 0.35; $p < 0.05$) and NW (R 0.25; $p < 0.10$) regimes, respectively, whereas weakly negative relationships are found for E and N weather types. Lastly, in autumn, the N (R 0.39; $p < 0.05$) and W (R 0.49; $p < 0.05$) weather types are the most positively correlated with DPWG, and the E and S regimes exhibit the most negative relationships. At monthly basis, the frequency (Figure 12a) and magnitude (Figure 12b) of wind gusts are positively and statistically significantly ($p < 0.05$) correlated with NW, W, SW, and N (i.e., directional weather types) denoting that extreme wind gust variability is driven by Atlantic large-scale synoptic flows, particularly during the cold semester (November–April). On the contrary, the frequency and magnitude of wind gusts is statistically significantly ($p < 0.05$)
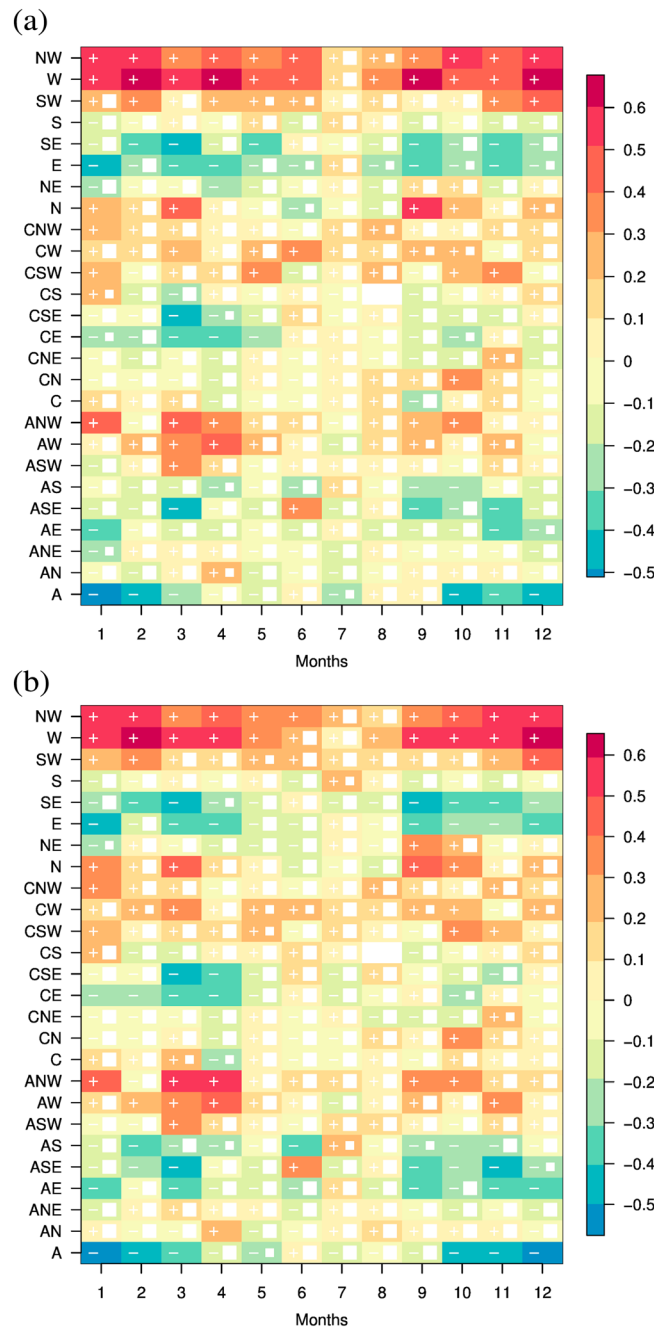
Figure 12. Monthly Pearson's correlation coefficients (R) between (a) the number of days exceeding the 54 year 90th DPWG percentile (frequency), and (b) the mean DPWG (magnitude) for the regional series, and the frequency series of the 26 Jenkinson and Collison weather types for 1961–2014. White squares mask the R not statistically significant at $p < 0.05$ (small squares) and $p < 0.10$ (big squares). The sign + or − of R is also shown.

inhibited under the A, ASE, CE, E, and SE regimes, i.e., anticyclonic and directional regimes from the Mediterranean region. Lastly, the long-term trend (1961–2014) of the major weather type (i.e., W as the primary driver of DPWG variability) indicates that this regime is the likely cause of the declining trends of winter and spring wind gusts (the occurrence of the W regime declined −0.414 and −0.201 d decade^{-1}, respectively; not significant at $p < 0.10$) and the increasing tendency of DPWG in summer and autumn (the W type increased +0.128 and +0.287 d decade^{-1}, respectively; also the NW type increased +0.374 d decade^{-1} in summer; not significant at $p < 0.10$).

4. Discussion

This study revealed long-term trends in the frequency and magnitude of daily peak wind gusts (DPWG) using homogenized anemometer observations from 80 stations across Spain and Portugal for 1961–2014. Overall, the annual frequency of DPWG declined (−1.49 d decade^{-1}), whereas a negligible negative (in essence nontrending) trend was observed in the annual magnitude of DPWG (−0.005 m s^{-1} decade^{-1}). More interestingly, we detected a distinct seasonal trend pattern with less frequent and declining DPWG episodes during the cold semester (November–April) and more frequent and increasing DPWG events during the warm semester (May–October). This marked seasonal monthly trend pattern suggests (i) a decreasing in the frequency of large-scale synoptic systems (e.g., extratropical cyclones) with weaker wind speed maxima affecting the IP during the cold semester and (ii) a strengthening of local wind circulations and/or extreme winds associated with deep mesoscale thun-

derstorms during the warm semester. A similar seasonal pattern characteristic of mean near-surface wind speed trends for the same region has been reported [*Azorin-Molina et al.*, 2014]. While consistent results between DPWG trends and mean near-surface wind speed trends are reported for the IP several other studies performed in different geographic regions detected differences in the reported trends by analyzing mean wind speed and wind speed maxima [*Klink*, 1999; *Vautard et al.*, 2010]. Our IP specific results agree with *Cabalar-Fuentes* [2005] for the northwestern part of the IP. These findings (i.e., agreement of trends for the IP versus contradictory trends

reported elsewhere [*Klink*, 1999; *Vautard et al.*, 2010] the latter having a focus on the entire northern hemisphere) demonstrate that local-to-regional weather systems and teleconnections with synoptic features (e.g., NAOI) are important to understanding wind dynamics for a study site the area of the IP.

The gradual evolution from negative (winter-spring) to positive (summer-autumn) trends in the frequency and magnitude of DPWG have not been previously reported in either hemisphere [*McVicar et al.*, 2012]. Our attribution analysis revealed that the less frequent and declining DPWG observed in winter is partly connected with the positive (yet not statistically significant at $p < 0.10$) trend experienced by the NAOI that is linked to an increase of anthropogenic forcings (e.g., greenhouse gases) [*Osborn*, 2011]. The tendency of positive NAOI phases is associated with a poleward shift of storms tracking across the Atlantic and the seasonal variations in the two poles of the NAOI, the Azores High, and the Icelandic Low [*Wang et al.*, 2011]. This stronger positive winter NAOI implies weaker westerly winds over this midlatitude region (e.g., southern Europe) dominated by the subtropical Azores high pressure belt but an increase of westerly and southwesterly winds associated with a steep pressure gradient between the subtropics and high latitudes and a strong polar jet stream over northcentral European latitudes [*Yan et al.*, 2002; *Smits et al.*, 2005]. In contrast, the negative and significant (at $p < 0.05$) trend of the NAOI in summer and autumn might be partly explaining the more frequent and increasing DPWG events experienced across the IP during the warm semester. *Wang et al.* [2011] described that in summer the IP lies in the southern periphery of the Azores High, where African easterly waves are impelled, favoring tropical cyclonegenesis and stormier summers. However, the NAOI-DPWG relationships found here are smaller in spring, summer, and autumn ($\sim -0.1 - -0.2$; $p > 0.10$), especially for the frequency, suggesting the hypothetical role of local-regional drivers on the reported increasing trends. For example, *Kim and Paik* [2015] hypothesized that Asian increasing summer wind speed is driven by intrusion of a warm air mass into the region (confirmed via increasing spatial variance in surface temperature). Moreover, the influence of the NAOI on the frequency and magnitude of damaging wind gusts has been previously discussed in two studies. First, *Pirazzoli and Tomasin* [2003] concluded that trends in mean and annual maximum winds in the central Mediterranean region are weakly correlated with the NAOI, being positively linked with air temperature. Second, *Cusack* [2013] concluded that about 20–30% of the variance in storm frequency in northern coastal Europe is explained by the NAOI.

Additionally, our secondary attribution analysis, by means of the Jenkinson and Collison weather-typing classification, also revealed the influence of large-scale atmospheric circulation on DPWG decadal variability. Among all 26 weather types, we found that the Westerly regime is the most positively and statistically significant ($p < 0.05$) correlated with the variability of extreme wind gusts; this means that westerly winds are the primary driver of the fastest wind speeds at most stations across Spain and Portugal. In accordance with this finding, but for Central Europe, *Donat et al.* [2010] concluded that 80% of storm days over that region are connected with westerly flows. Moreover, the long-term trends of DPWG are also consistent with the tendencies shown by the frequency of the Westerly regime, which has declined and increased (both not statistically significant at $p < 0.10$) during the cold and warm semesters, respectively. This reinforces our attribution analyses that highlights that the decadal variability of DPWG likely arises from changes in large-scale atmospheric circulation patterns as shown by the influence exerted by the NAOI and JC weather types, particularly during the cold semester (winter). This is very important as most severe wind extremes which represent a threat to human safety, maritime and aviation activities, and infrastructure, causing life and economic losses [*Della-Marta et al.*, 2009] are associated with large-scale synoptic disturbances in winter-spring seasons.

Vose et al. [2014] concluded that neither climate model projections nor our understanding of the physical climate system leads to any conclusive answers regarding extratropical cyclone activity given current climate change. For instance, the increasing trend in the frequency and magnitude of wind speed maxima during the warm semester seems to be a more complex phenomenon as DPWG in this semester are commonly weak-to-moderate winds associated with local-to-mesoscale processes across Spain and Portugal. Even though the relatively weak correlation was found between DPWG variability with the NAOI and JC weather types in summer and autumn, these positive DPWG trends likely reflect very complex interactions because wind speed maxima are mostly driven by thermal and friction forces instead of large-scale pressure gradient differences during these seasons [e.g., *Azorin-Molina et al.*, 2011; *Lorente-Plazas et al.*, 2015]. Lately, several studies [*Jerez et al.*, 2012; *Azorin-Molina et al.*, 2014; *Montávez et al.*, 2014] suggested that, for example, soil moisture depletion and other physical mechanisms are reinforcing the Iberian thermal low and therefore could be the cause of strengthening local wind circulations (e.g., sea breeze frontal passages) [*Azorin-Molina et al.*, 2011] and wind speed maxima during the warm semester. Changes in surface temperature may produce systematic changes

in surface winds [*Klink*, 1999; *Kim and Paik*, 2015] and therefore a global warming may have impacted the regional wind climate [*Yan et al.*, 2002]. In a global climate change scenario, the potential impact of increasing air temperature patterns on the frequency, duration, and magnitude of gusty winds and associated disasters must be further investigated. This requires looking at changes in both (i) large-scale atmospheric circulation patterns (e.g., poleward expansion of the Hadley cell) [*Lu et al.*, 2007] and (ii) local-to-mesoscale atmospheric dynamics (e.g., land-sea thermal contrast) such trends in the intensity of sea breezes and local wind circulations [*Azorin-Molina et al.*, 2011]. Therefore, a future attribution study aimed at revealing the physical causes behind the unexpected summer increases of both DPWG frequency and magnitude across the IP is required.

5. Conclusion

To summarize, the main findings of this long-term (1961–2014) trend study of daily peak wind gusts (DPWG) from 80 stations located across Spain and Portugal are:

1. The annual frequency of DPWG (90th percentile) statistically declined $-1.49 \, \text{d decade}^{-1}$ ($p < 0.05$) displaying a noticeable seasonal pattern with a significant ($p < 0.05$) decreasing trend in winter ($-0.75 \, \text{d decade}^{-1}$) and an increasing but not significant ($p < 0.10$) trend in summer ($+0.18 \, \text{d decade}^{-1}$).
2. The annual magnitude of DPWG (mean wind speed maxima) exhibited a slight declining trend ($-0.005 \, \text{m s}^{-1} \, \text{decade}^{-1}$; not significant at $p < 0.10$) but with marked seasonal differences between significant declining trends in winter ($-0.168 \, \text{m s}^{-1} \, \text{decade}^{-1}$; $p < 0.10$) and increasing trends in summer ($+0.130 \, \text{m s}^{-1} \, \text{decade}^{-1}$; $p < 0.05$).
3. Combining [1] and [2] reveals less frequent and declining DPWG during the cold semester (November–April) and more frequent and increasing DPWG during the warm semester (May–October).
4. Attribution analyses with the North Atlantic Oscillation Index (negative correlations $\sim -0.4 - -0.6$; $p < 0.05$) and the Jenkinson-Collison weather-typing classification (positive correlations mainly with Westerly regime: $\sim 0.5 - 0.6$; $p < 0.05$) show that variability of large-scale circulation is mostly driving the reported trends, particularly in winter. However, the NAOI-DPWG relationships are smaller in spring, summer, and autumn ($\sim -0.1 - -0.2$; $p > 0.10$), especially for the frequency.

References

Aguilar, E., I. Auer, M. Brunet, T. C. Peterson, and J. Wieringa (2003), Guidelines on Climate Metadata and Homogenization, 52 pp, World Meteorol. Organ, Geneva, Switzerland. [Available at http://www.wmo.int/datastat/documents/WCDMP-53_1.pdf, last accessed 1 November 2015.]

Alexander, L. V., S. F. B. Tett, and T. Jonsson (2005), Recent observed changes in severe storms over the United Kingdom and Iceland, *Geophys. Res. Lett.*, 32, L13704, doi:10.1029/2005GL022371.

Alexandersson, H. (1986), A homogeneity test to precipitation data, *Int. J. Climatol.*, 6(6), 661–675, doi:10.1002/joc.3370060607.

Ayala-Carcedo, F. J., and J. Olcina-Cantos (2002), *Riesgos Naturales* [in Spanish], 1512 pp., Ariel, Barcelona.

Azorin-Molina, C., D. Chen, S. Tijm, and M. Baldi (2011), A multi-year study of sea breezes in a Mediterranean coastal site: Alicante (Spain), *Int. J. Climatol.*, 31(3), 468–486, doi:10.1002/joc.2064.

Azorin-Molina, C., S. M. Vicente-Serrano, T. R. McVicar, S. Jerez, A. Sanchez-Lorenzo, J. I. López-Moreno, J. Revuelto, R. M. Trigo, J. A. Lopez-Bustins, and F. Espirito-Santo (2014), Homogenization and assessment of observed near-surface wind speed trends over Spain and Portugal, 1961–2011, *J. Clim.*, 27(10), 3692–3712, doi:10.1175/JCLI-D-13-00652.1.

Azorin-Molina, C., S. M. Vicente-Serrano, D. Chen, B. H. Connell, M. A. Domínguez-Durán, J. Revuelto, and J. I. López-Moreno (2015), AVHRR warm-season cloud climatologies under various synoptic regimes across the Iberian Peninsula and the Balearic Islands, *Int. J. Climatol.*, 35(8), 1984–2002, doi:10.1002/joc.4102.

Azorin-Molina, C., J.-A Guijarro, T. R McVicar, S. M. Vicente-Serrano, D. Chen, S. Jerez, and F. Espírito-Santo (2016), Trends of daily peak wind gusts in Spain and Portugal, *J. Geophys. Res. Atmos.*, 120, 1961–2014, doi:10.1002/2015JD024485.

Brázdil, R., K. Chromá, P. Dobrovolný, and R. Tolasz (2009), Climate fluctuations in the Czech Republic during the period 1961–2005, *Int. J. Climatol.*, 29(2), 223–242, doi:10.1002/joc.1718.

Cabalar-Fuentes, M. (2005), Los temporales de lluvia y viento en Galicia; Propuesta de clasificacion y analisis de tendencias (1961–2001) [in Spanish], *Invest. Geogr.*, 36, 103–118.

Cusack, S. (2013), A 101 year record of windstorms in the Netherlands, *Clim. Change*, 116(3), 693–704, doi:10.1007/s10584-012-0527-0.

Dadaser-Celik, F., and E. Cengiz (2014), Wind speed trends over Turkey from 1975 to 2006, *Int. J. Climatol.*, 34(6), 1913–1927, doi:10.1002/joc.3810.

Della-Marta, P. M., M. Hubert, F. Christoph, M. A. Liniger, J. Kleinn, and C. Appenzeller (2009), The return period of wind storms over Europe, *Int. J. Climatol.*, 29(39), 437–459, doi:10.1002/joc.1794.

Donat, M. G., G. C. Leckebusch, J. G. Pinto, and U. Ulbrich (2010), Examination of wind storms over Central Europe with respect to circulation weather types and NAO phases, *Int. J. Climatol.*, 30(9), 1289–1300, doi:10.1002/joc.1982.

Font-Tullot, I. (2000), *Climatologia de España y Portugal* [in Spanish], 422 pp., Universidad de Salamanca, Salamanca, Spain.

Fujii, T. (2007), On geographical distributions and decadal changes of the annual maximum wind speeds caused by typhoons in Japan, *J. Nat. Disaster Sci.*, 26(3), 267–277.

Grell, G. A., J. Dudhia, and D. R. Stauffer (1994), A description of the fifth-generation Penn State/NCAR Mesoscale Model (MM5), *NCAR Tech. Note 398 + STR*, Natl. Cent. For Atmos. Res, Boulder, Colo. [Available online at http://nldr.library.ucar.edu/collections/technotes/asset-000-000-000-214.pdf, last accessed 1 November 2015.]

Guijarro, J. A. (2011), Influence of network density on homogenization performance *Seventh Seminar for Homogenization and Quality Control in Climatological Databases* jointly organized with the Meeting of COST ES0601 (HOME) Action MC Meeting, Budapest, 24-27/October, WCDMP-No. 78, pp. 11–18.

Guo, H., M. Xu, and Q. Hu (2011), Changes in near-surface wind speed in China: 1969–2005, *Int. J. Climatol.*, *31*(3), 349–358, doi:10.1002/joc.2091.

Hewston, R., and S. R. Dorling (2011), An analysis of observed daily maximum wind gusts in the UK, *J. Wind Eng. Ind. Aerodyn.*, *99*(8), 845–856, doi:10.1016/j.jweia.2011.06.004.

Jenkinson, A. F., and B. P. Collison (1977), *An Initial Climatology of Gales Over the North Sea, Synoptic Climatol*. Branch Memo. 62 18 pp., Met Office, Bracknell, U. K.

Jerez, S., J. P. Montavez, J. J. Gomez-Navarro, P. A. Jiménez, P. Jimenez-Guerrero, R. Lorente-Plazas, and J. F. Gonzalez-Rouco (2012), The role of the land-surface model for climate change projections over the Iberian Peninsula, *J. Geophys. Res.*, *117*, D01109, doi:10.1029/2011JD016576.

Jerez, S., J. P. Montavez, P. Jimenez-Guerrero, J. J. Gomez-Navarro, R. Lorente-Plazas, and E. Zorita (2013), A multi-physics ensemble of present-day climate regional simulations over the Iberian Peninsula, *Clim. Dyn.*, *40*(11–12), 3023–3046, doi:10.1007/s00382-012-1539-1.

Jiang, Y., Y. Luo, Z. Zhao, and S. Tao (2010), Changes in wind speed over China during 1956–2004, *Theor. Appl. Climatol.*, *99*(3–4), 421–430, doi:10.1007/s00704-009-0152-7.

Jones, P. D., T. Jonsson, and D. Wheeler (1997), Extension to the North Atlantic Oscillation using early instrumental pressure observations from Gibraltar and South-West Iceland, *Int. J. Climatol.*, *17*(13), 1433–1450, doi:10.1002/(SICI)1097-0088(19971115)17:13<1433::AID-JOC203>3.0.CO;2-P.

Kendall, M. G., and J. D. Gibbons (1990), *Rank Correlation Methods*, 272 pp., Oxford Univ. Press, New York.

Khaliq, M. N., and T. B. M. J. Ouarda (2007), On the critical values of the standard normal homogeneity test (SNHT), *Int. J. Climatol.*, *27*(5), 681–687, doi:10.1002/joc.1438.

Kim, J., and K. Paik (2015), Recent recovery of surface wind speed after decadal decrease: A focus on South Korea, *Clym. Dyn.*, *45*(5), 1699–1712, doi:10.1007/s00382-015-2546-9.

Klink, K. (1999), Trends in mean monthly maximum and minimum surface wind speeds in the coterminous United States, 1961 to 1990, *Clim. Res.*, *13*(3), 193–205, doi:10.3354/cr013193.

Klink, K. (2015), Seasonal patterns and trends of fastest 2-min winds at coastal stations in the conterminous USA, *Int. J. Climatol.*, *35*(14), 4167–4175, doi:10.1002/joc.4275.

Kruger, A. C., A. M. Goliger, J. V. Retief, and S. Sekele (2010), Strong wind climatic zones in South Africa, *Wind Struct.*, *13*(1), 37–55.

Livezey, R. E., and W. Y. Chen (1983), Statistical field significance and its determination by Monte Carlo techniques, *Mon. Weather Rev.*, *111*(1), 46–59, doi:10.1175/1520-0493(1983)111<0046:SFSAID>2.0.CO;2.

Lorente-Plazas, R., J. P. Montávez, S. Jerez, J. J. Gómez-Navarro, P. Jiménez-Guerrero, and P. A. Jiménez (2015), A 49 year hindcast of surface winds over the Iberian Peninsula, *Int. J. Climatol.*, *35*(10), 3007–3023, doi:10.1002/joc.4189.

Lu, J., G. A. Vecchi, and T. Reichler (2007), Expansion of the Hadley cell under global warming, *Geophys. Res. Lett.*, *34*, L06805, doi:10.1029/2006GL028443.

Martin-Vide, J., and J. Olcina-Cantos (2001), *Climas y Tiempos en España* [in Spanish], 264 pp., Alianza Ed.

McVicar, T. R., T. G. Van Niel, L. T. Li, M. L. Roderick, D. P. Rayner, L. Ricciardulli, and R. J. Donohue (2008), Wind speed climatology and trends for Australia, 1975–2006: Capturing the stilling phenomenon and comparison with near-surface reanalysis output, *Geophys. Res. Lett.*, *35*, L20403, doi:10.1029/2008GL035627.

McVicar, T. R., T. G. Van Niel, M. L. Roderick, L. T. Li, X. G. Mo, N. E. Zimmermann, and D. R. Schmatz (2010), Observational evidence from two mountainous regions that near-surface wind speeds are declining more rapidly at higher elevations than lower elevations: 1960–2006, *Geophys. Res. Lett.*, *37*, L06402, doi:10.1029/2009GL042255.

McVicar, T. R., et al. (2012), Global review and synthesis of trends in observed terrestrial near-surface wind speeds: Implications for evaporation, *J. Hydrol.*, *416–417*, 182–205, doi:10.1016/j.jhydrol.2011.10.024.

Mescherskaya, A. V., V. V. Eremin, A. A. Baranova, and V. V. Maystrova (2006), Change in wind speed in northern Russia in the second half of the twentieth century, from surface and upper air data [in Russian], *Russ. Meteorol. Hydrol.*, *9*, 46–58.

Montávez, J. P., R. Lorente-Plazas, S. Jerez, P. Jiménez-Guerrero, J. A. García-Valero, and P. A. Jiménez (2014), Climatología del viento sobre la Península Ibérica: Observaciones y modelos [in Spanish], in *Cambio Climático y Cambio Global*, vol. 9, edited by S. Fernandez-Montes and F. S. Rodrigo, pp. 675–685, Asociación Española de Climatología, Almería, Spain.

Osborn, T. J. (2011), Variability and changes in the North Atlantic Oscillation Index, in *Hydrological, Socieconomic and Ecological Impacts of the North Atlantic Oscillation in the Mediterranean region*, *Adv. Global Change Res.*, vol. 46, edited by S. M. Vicente-Serrano and R. M. Trigo, pp. 9–22, Springer, Netherlands.

Péliné Németh, C., K. Radics, and J. Bartholy (2011), Seasonal variability of wind climate in Hungary, *Acta Silvatica Lignaria Hung.*, *7*, 39–48.

Pirazzoli, P. A., and A. Tomasin (2003), Recent near-surface wind changes in the central Mediterranean and Adriatic areas, *Int. J. Climatol.*, *23*(8), 963–973, doi:10.1002/joc.925.

Pryor, S. C., R. J. Barthelmie, D. T. Young, E. S. Takle, R. W. Arritt, D. Flory, W. J. Gutowski Jr., A. Nunes, and J. Roads (2009), Wind speed trends over the contiguous United States, *J. Geophys. Res.*, *114*, D14105, doi:10.1029/2008JD011416.

Roderick, M. L., L. D. Rotstayn, G. D. Farquhar, and M. T. Hobbins (2007), On the attribution of changing pan evaporation, *Geophys. Res. Lett.*, *34*, L17403, doi:10.1029/2007GL031166.

Smits, A., A. M. G. Klein-Tank, and G. P. Können (2005), Trends in storminess over the Netherlands, 1962–2002, *Int. J. Climatol.*, *25*(10), 1331–1344, doi:10.1002/joc.1195.

Spellman, G. (2000), The application of an objective weather-typing system to the Iberian peninsula, *Weather*, *55*(10), 375–385, doi:10.1002/j.1477-8696.2000.tb04023.x.

Sweeney, J. (2000), A three-century storm climatology for Dublin 1715–2000, *Irish Geogr.*, *33*(1), 1–14, doi:10.1080/00750770009478595.

Ulbrich, U., and M. Christoph (1999), A shift of the NAO and increasing storm track activity over Europe due to anthropogenic greenhouse gas forcing, *Clim. Dyn.*, *15*, 551–559, doi:10.1007/s003820050299.

Usbeck, T., T. Wohlgemuth, M. Dobbertin, C. Pfister, A. Bürgi, and M. Rebetez (2010), Increasing storm damage to forests in Switzerland from 1858 to 2007, *Agric. For. Meteorol.*, *150*(1), 47–55, doi:10.1016/j.agrformet.2009.08.010.

Vautard, R., J. Cattiaux, P. Yiou, J.-N. Thépaut, and P. Ciais (2010), Northern Hemisphere atmospheric stilling partly attributed to an increase in surface roughness, *Nat. Geosci.*, *3*(11), 756–761, doi:10.1038/ngeo979.

Venema, V. K. C., et al. (2012), Benchmarking homogenization algorithms for monthly data, *Clim. Past*, *8*(1), 89–115, doi:10.5194/cp-8-89-2012.

Vicente-Serrano, S. M., and R. M. Trigo (2011), Hydrological, socioeconomic and ecological impacts of the North Atlantic Oscillation in the Mediterranean region, in *Advances in Global Change Research*, vol. 46, 236 pp., Springer, NetherLands.

von Storch, H. (1995), Misuses of statistical analysis in climate research, in *Analysis of Climate Variability: Applications of Statistical Techniques*, edited by H. von Storch and A. Navarra, pp. 11–26, Springer.

Vose, R. S., et al. (2014), Monitoring and understanding changes in extremes: Extratropical storms, winds, and waves, *Bull. Am. Meteorol. Soc.*, *95*(3), 377–386, doi:10.1175/BAMS-D-12-00162.1.

Wan, H., L. W. Xiaolan, and V. R. Swail (2010), Homogenization and trend analysis of Canadian near-surface wind speeds, *J. Clim.*, *23*(5), 1209–1225, doi:10.1175/2009JCLI3200.1.

Wang, X., H. Wan, F. W. Zwiers, V. R. Swail, G. P. Compo, R. J. Allan, R. S. Vose, S. Jourdain, and X. Yin (2011), Trends and low-frequency variability of storminess over western Europe, 1878–2007, *Clim. Dyn.*, *37*(11), 2355–2371, doi:10.1007/s00382-011-1107-0.

Weatherhead, E. C., et al. (1998), Factors affecting the detection of trends: Statistical considerations and applications to environmental data, *J. Geophys. Res.*, *103*(D14), 17,149–17,161, doi:10.1029/98JD00995.

Wilks, D. S. (2006), On "field significance" and the false discovery rate, *J. Appl. Meteorol. Climatol.*, *45*(9), 1181–1189, doi:10.1175/JAM2404.1.

WMO (1987), The measurement of gustiness at routine wind stations: A review, (A.C.M. Beljaars), *Instruments and Observing Methods Report* No. 31, Geneva.

WMO (2008), *Guide to Meteorological Instruments and Methods of Observation*, *World Meteorol. Organ*. No. 8, 7th. [Available at http://www.wmo.int/pages/prog/gcos/documents/gruanmanuals/CIMO/CIMO_Guide-7th_Edition-2008.pdf], (last accessed 1 November 2015). ed., Geneva, Switzerland.

Xu, M., C. P. Chang, C. Fu, Y. Qi, A. Robock, D. Robinson, and H. Zhang (2006), Steady decline of east Asian monsoon winds, 1969–2000: Evidence from direct ground measurements of wind speed, *J. Geophys. Res.*, *111*, D24111, doi:10.1029/2006JD007337.

Yan, Z., S. Bate, R. E. Chandler, V. Isham, and H. Wheater (2002), An analysis of daily maximum wind speed in northwestern Europe using generalized linear models, *J. Clim.*, *15*(15), 2073–2088, doi:10.1175/1520-0442(2002)015<2073:AAODMW>2.0.CO;2.